Electronic Supplementary Material (ESI) for Green Chemistry.
This journal is © The Royal Society of Chemistry 2015

Supporting Information

Removal and safe reuse of highly toxic allyl alcohol by highly selective photo-sensitive metal-organic framework

Feng Luo,[1]*Le Le Gong,[1] Xue Feng Feng,[1] Xian Feng Yi,[2] and An Min Zheng*[2]

Table S1. The EA and TG results in this work

Compounds	EA	TG
$Zn(L)(bpe)\cdot(H_2O)_3(DMF)_{1.5}$	calc. C/49.41, N/10.38, H/4.42 exp. C/49.23, N/10.31, H/4.36	At 35-320°C, loss all solvents exp. 21.8%, calc. 22.1%
$Zn(L)(bpe)\cdot(DMF)_{1.2}$	calc. C/53.42, N/10.94, H/3.69 exp. C/53.49, N/10.89, H/3.72	At 35-275°C, loss all solvents exp. 13.2%, calc. 13.2%
$Zn(L)(bpa)_{0.5}(bpe)_{0.5}\cdot(DMF)_{1.2}$	calc. C/53.78, N/10.48, H/3.97 exp. C/53.72, N/10.41, H/3.92	At 35-230°C, loss all solvents exp. 13.2%, calc. 13.2%; At 230-285°C, cleavage of cyclobutane rings and release of allyl alcohol, exp. 4.3%, calc. 4.2%

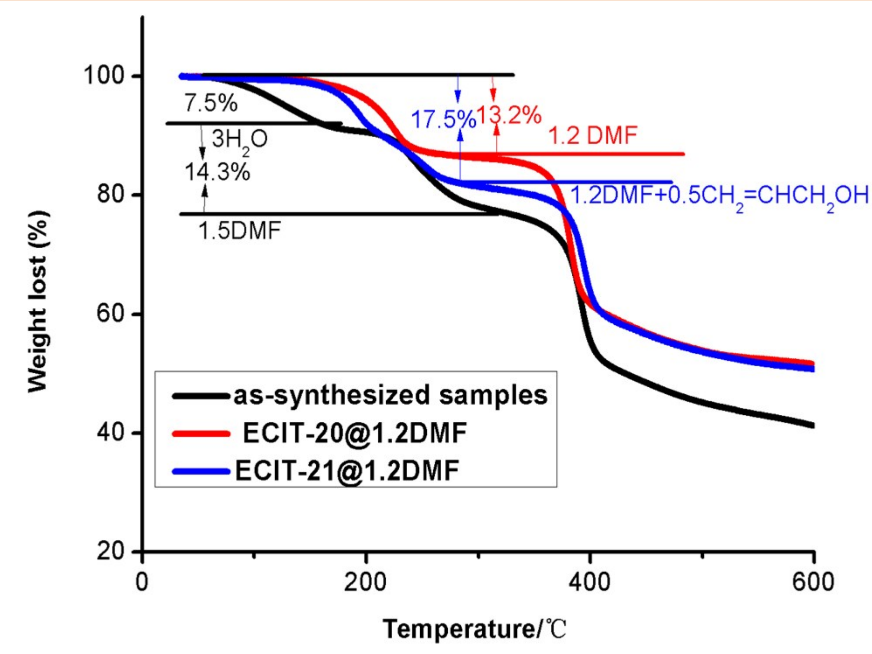

Figure S1. The TG plots in this work.

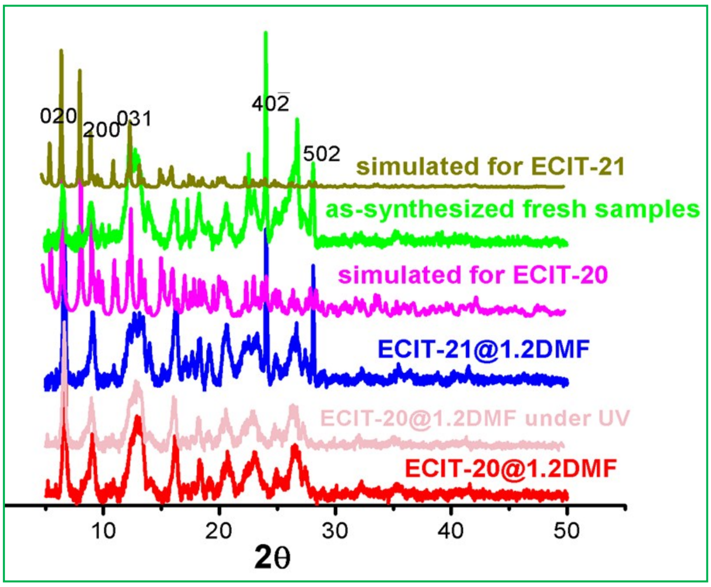

Figure S2. The PXRD patterns in this work.

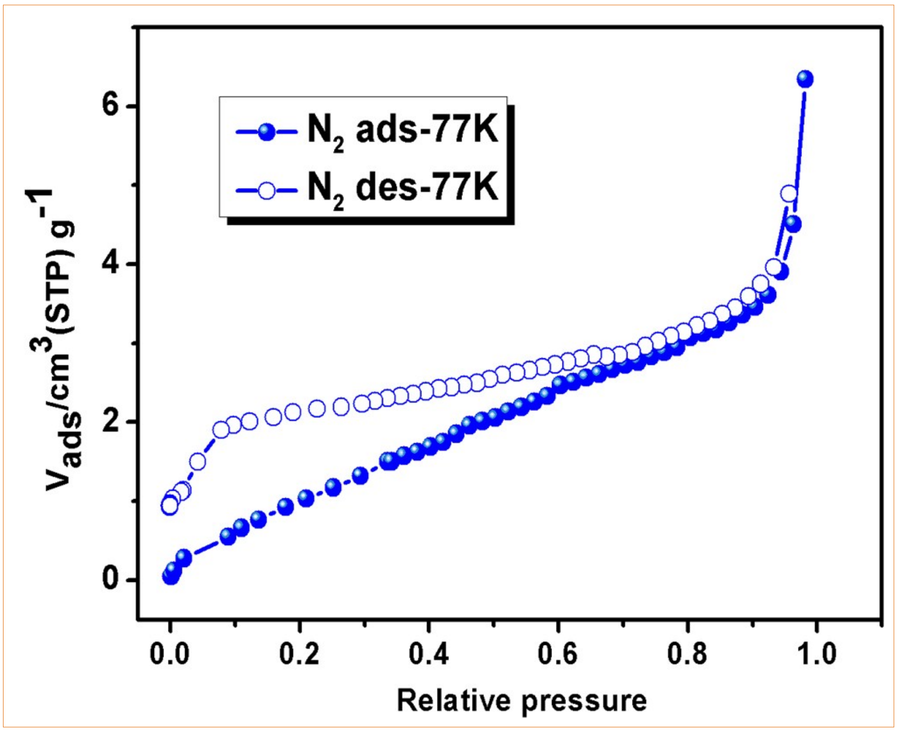

Figure S3. The N_2 adsorption isotherm at 77K for **ECIT-20@1.2DMF**.

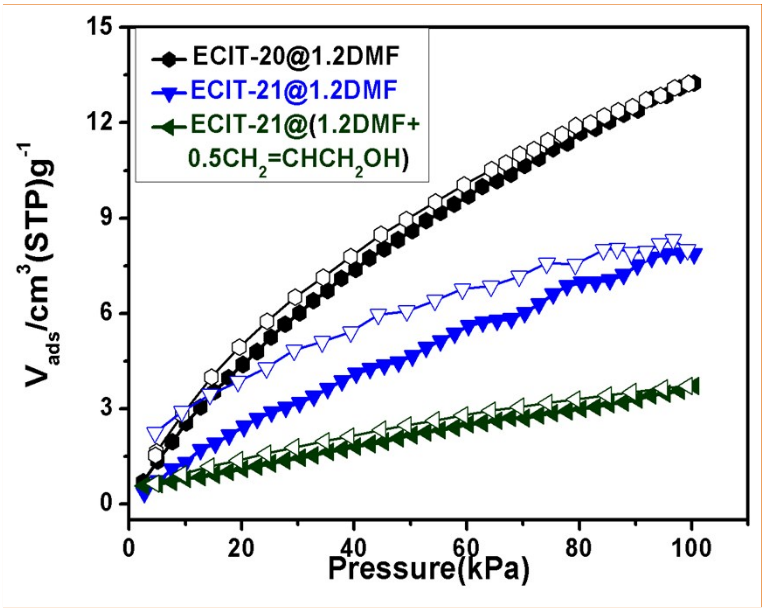

Figure S4. The CO_2 adsorption isotherms at 293 K for **ECIT-20@1.2DMF**, **ECIT-21@1.2DMF**, and **ECIT-21@(1.2DMF+0.5CH_2=$CHCH_2OH$)**, respectively. **ECIT-21@(1.2DMF+0.5CH_2=$CHCH_2OH$)** was obtained in this way that **ECIT-20@1.2DMF** underwent CH_2=$CHCH_2OH$ adsorption under UV but without desorption. Note: adsorption (solid symbols) and desorption (open symbols).

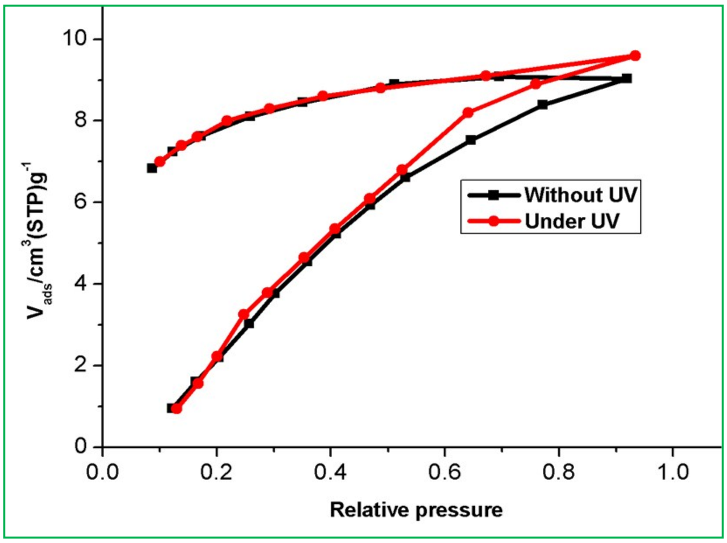

Figure S5. C_2H_5OH adsorption isotherms on **ECIT-20@1.2DMF** at 298K with UV or without UV, respectively.

Solid-State NMR. It was performed at room temperature on a Bruker DRX400-WB instrument. Chemical shifts were referred to external standard adamantane. The broadness would due to chemical shift anisotropy, dipolar and quadrupolar interactions, etc., which was averaged by faster MAS spinning. Due to overlapping and broadening of the signals, complete assignment of chemical shifts was not attempted.

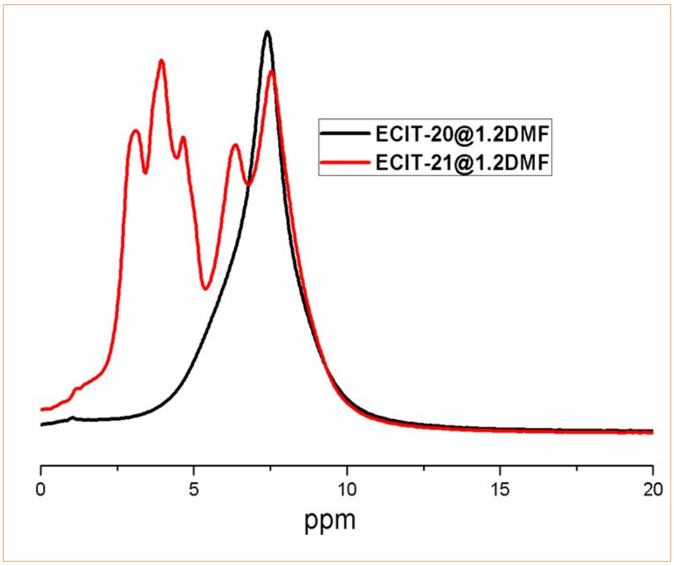

Figure S6. ^{1}H MAS solid-state NMR spectrum of **ECIT-20@1.2DMF** and **ECIT-21@1.2DMF.** The overlapping and broadening of the signals at 2.3-11.5 ppm in **ECIT-20@1.2DMF** is due to DMF, bpe and L ligand. The signals at 3.1 ppm, 3.9 ppm, 4.6 ppm is due to DMF and cyclobutane segment. The signals at 6.4 ppm resulted from partly bpa pyridyl hydrogen atoms close to the cyclobutane segment. The signals at 7.4 ppm resulted from partly bpa pyridyl hydrogen atoms close to the pyridyl nitrogen atom plus L hydrogen atoms.

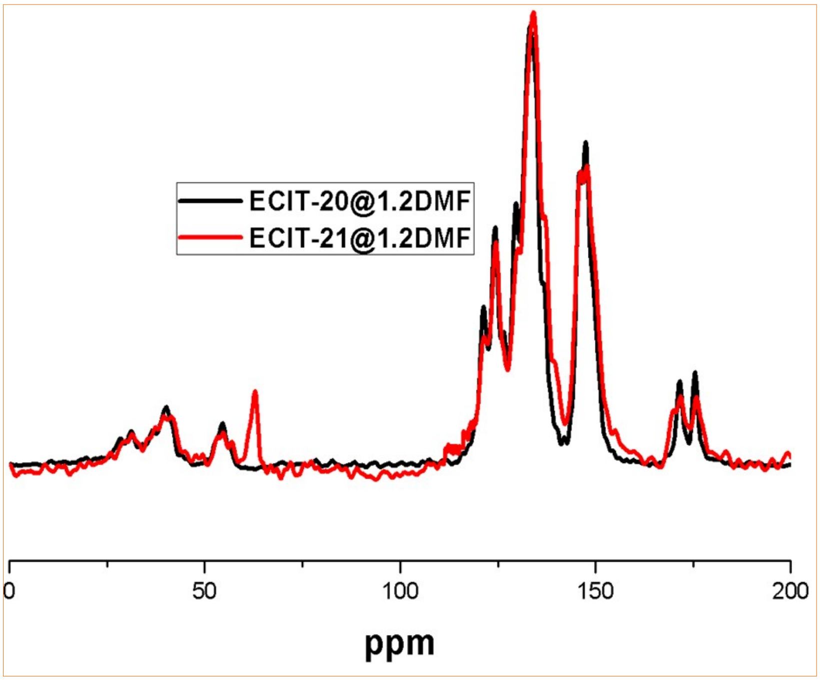

Figure S7. ^{13}C CPMAS solid-state NMR spectrum of **ECIT-20@1.2DMF** and **ECIT-21@1.2DMF.** The signals at 171.2 ppm and 176.2 ppm is derived from DMF C=O fragment and L carboxylate. The peaks at 147.2 ppm, 134.0 ppm, 124.3 ppm 121.3 ppm is due to the bpe, L carbon atoms in **ECIT-20@1.2DMF** and bpe, bpa, L carbon atoms in **ECIT-21@1.2DMF**. The peak at 129.4 ppm is assigned to C=C of bpe. Peak at 62.8 ppm should be CH_2OH carbon atoms of cyclobutane segment in **ECIT-21@1.2DMF**. And the small humps at 24-59 ppm is due to DMF and cyclobutane.

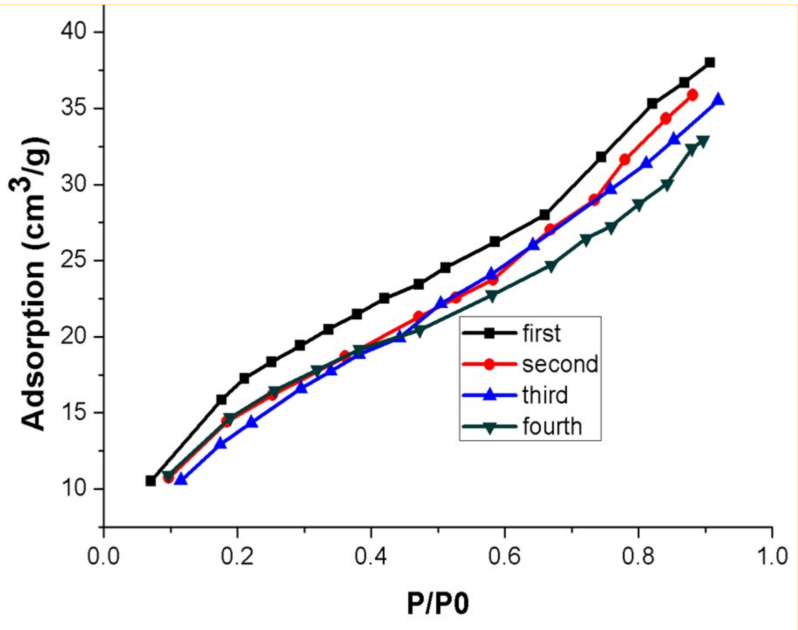

Figure S8. The capture/release cycle obtain in this way, photochemical [2+2] cycloaddition for capture allyl alcohol and thermo-dependent reversible cleavage of cycloaddition for release of allyl alcohol. The samples were prepared in detail as follows: **ECIT-20@1.2DMF** is used to capture allyl alcohol under UV, then the release is by heating the samples after loading allyl alcohol at 285°C for 24 h.

Hg^{2+} adsorption. A stock solution of Hg(II) (1000 mg L^{-1}) was prepared from $Hg(NO_3)_2$. All the working Hg(II) solutions were prepared using appropriate subsequent dilutions of the stock solution. The adsorption of Hg(II) was carried out under static conditions. The pH of Hg(II) solution was adjusted to the required value by HCl and $NH_3 \cdot H_2O$ solutions. The residual concentration of the Hg^{2+} in the solution was determined by the atomic fuorescence spectrometer (AFS). The amount of adsorption at equilibrium, qe (mg g^{-1}), was calculated according to eqn (1):

$$q_e = \frac{(c_0 - c_e)v}{m} \qquad (1)$$

Where c_0 (mg L^{-1}) and c_e(mg L^{-1}) are the initial and equilibrated concentrations of Hg^{2+}, respectively, v (L) is the volume of solution, and m (g) is the mass of dry adsorbent. The removal efficiency (%) of the mercury was calculated by Eq. (2):

$$\text{Removal efficiency (\%)} = \frac{c_0 - c_e}{c_0} \times 100\% \qquad (2)$$

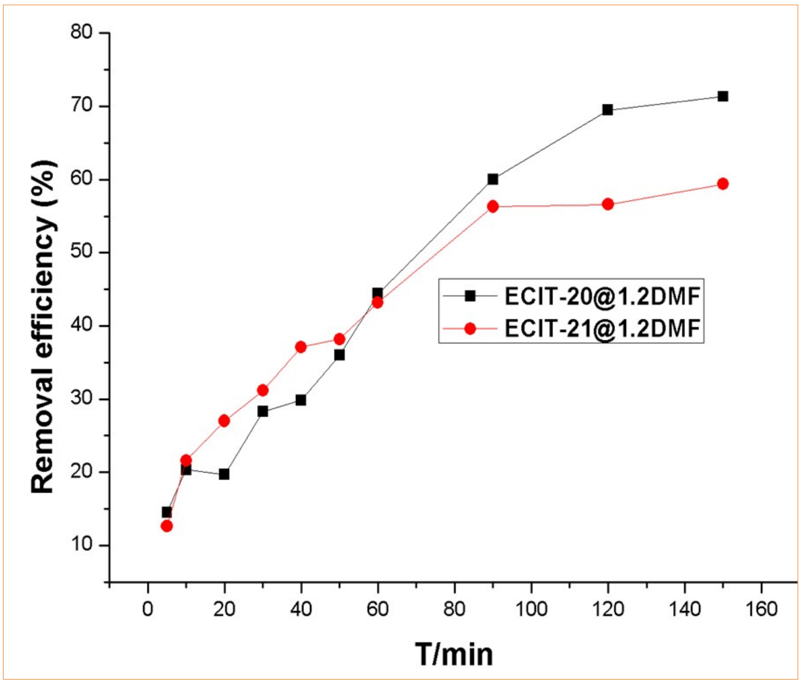

Figure S9. Effect of contact time on Hg^{2+} removal ($c_0(Hg^{2+})$=100 ppb, v=10 mL, m(adsorbent)=2 mg, T=25℃, pH=7).

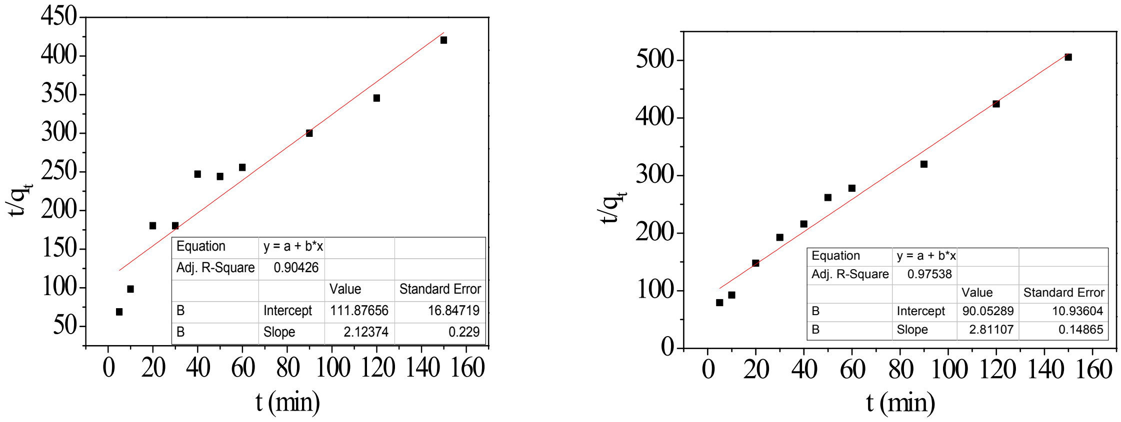

Figure S10. The fitting of pseudo-second-order kinetic plot for the adsorption of Hg^{2+} onto **ECIT-20@1.2DMF**/left and **ECIT-21@1.2DMF**/right, respectively. Note: The pseudo-second-order model is expressed as

$$\frac{t}{q_t} = \frac{1}{k_2 q_e^2} + \frac{t}{q_e}$$

where k_2 (g (mg min^{-1})) is the pseudo-second-order rate constant, q_e(mg g^{-1}) and q_t (mg g^{-1}) are the adsorption amounts at equilibrium and at time t, respectively. The fitting results were listed as follows: for **ECIT-20@1.2DMF,** k_2=0.04(g/(mg· min)), q_e=0.4709mg/g, $q_{exp.}$=0.3568mg/g; for **ECIT-21@1.2DMF,** k_2=0.0878(g/(mg· min)), q_e=0.3557mg/g, $q_{exp.}$= 0.2967mg/g.

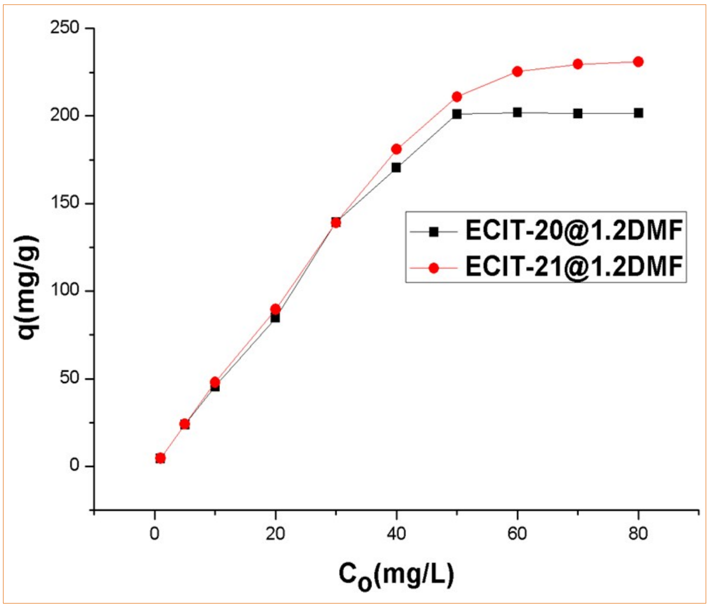

Figure S11. Sorption isotherm of $Hg^{2+}$for **ECIT-20@1.2DMF** and **ECIT-21@1.2DMF**(v=10 mL, m(adsorbent)=2 mg, T=25℃, t=150 min, pH=7).

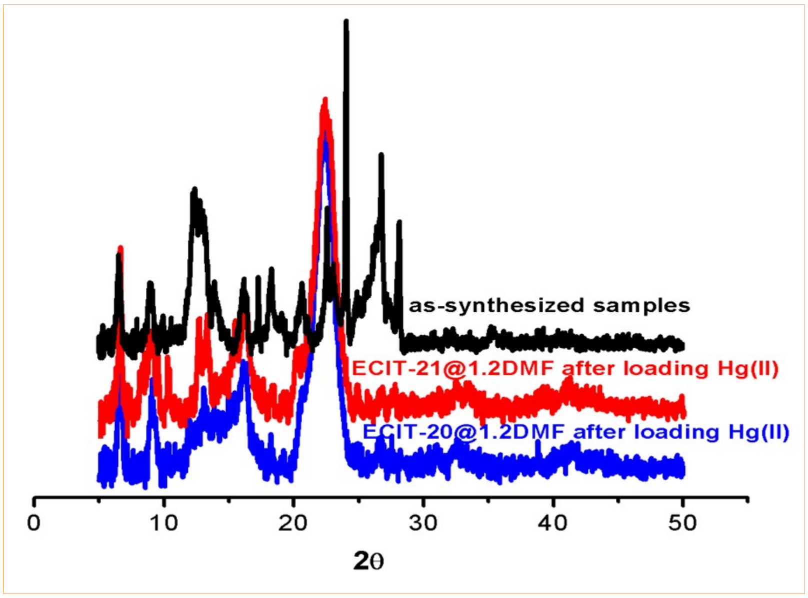

Figure S12. PXRD patterns for the samples of **ECIT-20@1.2DMF** and **ECIT-21@1.2DMF** after loading Hg(II). It is clear that their PXRD patterns match well with the as-synthesized samples, indicating that the skeleton integrity can be maintained even after loading Hg(II). The enhanced and sharp peak at 2θ=22.4 indicates the formation of a more dense phase after loading Hg(II).